

ORIGINAL PAPER

Characterization and Antifungal Efficacy of Biogenic Silver Nanoparticles and Silver–Chitosan Nanocomposites

Mahmoud, M.A. 

Received: 22 September 2021 / Accepted: 27 October 2021 / Published online: 28 October 2021.
©Egyptian Phytopathological Society 2021

ABSTRACT

The present study aimed for a comparative study of green protocol for the biogenic synthesis of silver nanoparticles (AgNPs) and silver-chitosan nanocomposites (Ag-CS-NCs), characterization, and comparative evaluation of antifungal and anti-aflatoxin B1 activity potentials of both nanoparticles (NPs). The cell-free culture filtrate (CFF) of *Aspergillus terreus* (KC462061) was utilized to biogenic synthesis AgNPs and Ag-CS-NCs. The physicochemical characterization was done by ultraviolet-visible spectroscopy (UV-Vis), transmission electron microscopy (TEM), high-resolution scanning electron microscopy (HR-SEM), Energy Dispersive Spectroscopy (EDS), Fourier transform-infrared spectroscopy (FTIR). The UV-Vis spectroscopy of the prepared AgNPs and Ag-CS-NCs showed variation in the appearance of specific significant peaks, 425 nm for AgNPs and 275, 425 nm for Ag-CS-NCs. The microscopic analysis was done by TEM and the results revealed that both NPs were spherical in shape, with average size ranged from 10 to 60 nm. The HR-SEM micrographs revealed a rough surface with uneven surface topology of the AgNPs, while Ag-CS-NCs were thin, straight and smooth pipe. FTIR spectroscopy indicated that the functional groups (proteins and secondary metabolites) present in the CFF might be responsible for the bioreduction of Ag⁺ (ions) to produce stabilized protein-capped AgNPs. This study presents the antifungal activity and anti-aflatoxin B1 of AgNPs and Ag-CS-NCs against an aflatoxigenic isolates of *A. flavus*. Our *in vitro* results showed notable antifungal activity and potency in thwarting aflatoxin B1 (AB1) production. In addition, SEM imaging was applied to observe the changes in fungal hyphal morphological features after the interactions with AgNPs and Ag-CS-NCs.

Keywords: Silver nanoparticles, Silver-chitosan nanocomposites, Antifungal activity, Anti-Aflatoxin B1.

*Correspondence: Mahmoud, M.A.

E-mail: m.a.mahmoud75@gmail.com

Mohamed A. Mahmoud

 <https://orcid.org/0000-0003-3940-5753>

Plant Pathology Research Institute,
Agricultural Research Center, 12619, Giza,
Egypt.

INTRODUCTION

The contamination of agricultural products with aflatoxins is a major problem for economic and public health. Aflatoxins (AFs) are fungal subsidiary products mainly developed by *Aspergillus flavus* isolates on human food and animal feed under warm and humid conditions (Omeiza *et al.*, 2018). The significant source of AFs spoilage is *A. flavus*, especially AB1, which has received a lot of attention in the food and feed industry (Li *et al.*, 2019). In the recent decades, several researchers focused on biological control strategies effective in reducing mycotoxigenic fungi during storage and their mycotoxins. However, chemical control is still considered a key tool to limit fungal diseases on many important food crops (Abdallah *et al.*, 2018). Also, current disease management for fungal diseases relies heavily on the application of

fungicides in spite of many advantages, but there are many side effects like non-target organisms, the resurgence of the pest population and the development of resistance (Stephenson, 2003). Furthermore, it is estimated that 90% of applied pesticides are lost during or after application. As a result, there is an increased motivation to develop cost-efficient, high-performing fungicides, that being less harmful to the environment (Ghormade *et al.*, 2011). Nanotechnology has led to the development of new concepts of plant disease management with immense potential to manage the aforementioned problems (Balaure *et al.*, 2017). Nanoparticles have benefited the area of crop and food protection due to the development of new antifungal agents, particularly for the decline using of chemicals fungicides. Additionally, nanosensors were developed for plant health and monitoring the food contaminants (e.g., fungicide) to guarantee food quality and safety (Kim *et al.*, 2018). AgNPs are one of the most orderly studied nanomaterials which have extremely powerful against plant pathogenic fungi lead to a broad range of applicability in fungicidal activity (Worrall *et al.*, 2018). Therefore, the effort has been given for the establishment of a novel biomaterial consisted of

AgNPs embedded in a polymer network (AgNPs/polymer nanocomposites) are perfect as antimicrobial substances which have been used in the management of fungal plant pathogens and food packing (Jung *et al.*, 2018). Silver-chitosan nanocomposites (Ag-CS-NCs) have been examined for the control of some fungal plant pathogens. Kaur *et al.* (2012) observed notable antifungal activity against *Alternaria alternata*, *Aspergillus flavus* and *Rhizoctonia solani*. The antifungal activity of AgNPs against *Aspergillus flavus* and AgNPs in inhibiting the production of AFB1 appeared very promising case as antifungal activity and anti-aflatoxin B1 production (Al-Othman *et al.*, 2014; Al-Zaban *et al.*, 2021).

The main aim of the current study was to 1) biogenic synthesize AgNPs and Ag-CS-NCs and characterize using the cell-free culture filtrate of *Aspergillus terreus* (KC462061) 2) create a characterization for the AgNPs and Ag-CS-NCs ultraviolet-visible spectroscopy (UV-Vis), transmission electron microscopy (TEM), high-resolution scanning electron microscopy (HR-SEM), Energy Dispersive Spectroscopy (EDS), Fourier transform-infrared spectroscopy (FTIR) 3) evaluate the antifungal and anti-aflatoxin B1 activity of AgNPs and Ag-CS-NCs against some *A. flavus* toxigenic isolates.

MATERIALS AND METHODS

Fungal isolate source:

Aspergillus terreus (KC462061), registered in GenBank by Abd El-Aziz *et al.* (2013). *Aspergillus terreus* (KC462061) was isolated from soil cultivated with date palm.

Aspergillus flavus source:

Three aflatoxigenic *Aspergillus flavus* isolates included isolate no. C12 low producer (LP), C6 intermediate producer (IP), and C8 high producer (HP) were isolated from corn grain. These *A. flavus* isolates were previously identified by Mahmoud *et al.* (2014). These isolates were used in antifungal and antiaflatoxigenic activities experiments.

Biogenic of AgNPs:

Biomass Preparation:

In brief, to prepare biomass for biosynthesis studies, the fungus was grown in 250 mL Erlenmeyer flasks containing 100 mL liquid medium containing KH_2PO_4 , K_2HPO_4 , $\text{MgSO}_4 \cdot 7\text{H}_2\text{O}$, $(\text{NH}_4)_2\text{SO}_4$, yeast extract, and glucose. The flask was incubated in a shaker at 150 rpm. After three days of growth, the fungal mycelium biomass was harvested by sieving

through a Whatman filter paper no.1, followed by inclusive washing with deionized water to remove any particle of medium adhering to the fungal biomass (Sadowski *et al.*, 2008).

Biogenic synthesis of AgNPs:

The aqueous solution containing 0.001 M silver nitrate was prepared, added to the cell-free filtrate in the reaction flask (1:1), and incubated in the rotary shaker at 28 °C (150 rpm) in the dark. The reaction mixture was incubated (72 hours) until the color shifts from light yellow to dark brown. A powder of the AgNPs was obtained after transferring AgNPs solution to the freeze-dryer at -20 °C under vacuum to eliminate the water from the AgNPs solution. The control contains silver nitrate solution (without cell-free filtrate). The control showed no apparent change in color. All treatments were replicated (Sadowski *et al.*, 2008).

Biosynthesis of silver-chitosan nanocomposites (Ag-CS-NCs):

Ag-CS-NCs compound was prepared using AgNPs and chitosan (CS) as a reducing and stabilizing agent. a fresh aqueous chitosan, ($\geq 75\%$ degree of deacetylation, Cat No. C3646, Sigma-Aldrich). 0.2 grams of chitosan were dissolved in 10 ml of CH_3COOH solution (1% v/v). After mixing chitosan solution with silver nanoparticle suspension (1:2 v/v), this was stirred continually for 30-45 minutes, then, AgNPs – chitosan mixture solution was achieved. The mixture solution was then dropped into a 25 mL NaOH solution with different concentrations (20%, 30%, or 40%) using a syringe pump. After 15 minutes, Ag-CS-NCs were obtained (light brown color). Nanoparticles were collected and washed twice with 50 mL of dd- H_2O to eliminate residual alkali (Wang *et al.*, 2015).

Characterization of AgNPs and Ag-CS-NCs:

UV-Visible spectral analysis:

The use of UV-Vis spectrophotometry technique to confirm the formation of AgNPs and Ag-CS-NCs was carried out using a double-beam UV-Vis spectrophotometer at wavelengths between 200 to 800 nm, GBC Cintra 10 (GBC Scientific Equipment, Australia), depends on the color variation of the reaction mixture observed by absorption spectra (Wang *et al.*, 2015 and Raza *et al.*, 2021).

Transmission electron microscopy (TEM):

TEM was performed on JEOL, JEM-1400 (Tokyo, Japan) instrument, with an accelerating voltage of 100 kV after drying of a drop of aqueous both biosynthesized nanoparticles on the carbon-coated copper TEM grids. Samples were dried and kept under vacuum in desiccators

before loading them onto a specimen holder. The particle size distribution of silver nanoparticles was evaluated using Image J 1.45s software (1493). The TEM technique was carried out exactly as (Musarrat *et al.*, 2010).

High-resolution scanning electron microscopy (HR-SEM) and energy dispersive X-ray (EDS):

The biosynthesized AgNPs and Ag-CS-NCs were subjected to HR-SEM JEOL, JSM-7610F (Tokyo, Japan), and EDS (the same equipment) were used to examine the morphology, size, and pattern detection of the fundamental elements of nanomaterials.

Nanoparticles functional groups analysis:

Analysis of both biosynthesized nanoparticles particularly functional groups in the scanning ranges from 400 to 4000 cm^{-1} at a resolution of 4 cm^{-1} was carried out using Fourier-Transform Infrared (FTIR) spectroscopy Thermo Fisher, Nicolet 6700 (Massachusetts, USA) (Griffiths and de Haseth, 2007).

Antifungal activity of AgNPs and Ag-CS-NCs:

The antifungal activities of AgNPs and Ag-CS-NCs were examined *in vitro* against *A. flavus*. The antifungal activity is based on the reduction in fungal growth of the three isolates of *A. flavus* using the agar well diffusion method (Savi *et al.*, 2012). Different concentrations (0.3, 0.5, 0.7 and 1 mM) of both AgNPs and Ag-CS-NCs were used. In the center of each Petri plate containing the potato dextrose agar (PDA) a disc (6 mm in diameter) of mycelia taken from the edges of 7-day-old *A. flavus* cultures was seeded. A sterile cork borer (0.6 cm diameter) was used to punching PDA to make open wells. AgNPs and Ag-CS-NCs were added into the open wells with different concentrations. The plates were incubated at $28 \pm 2^\circ\text{C}$ for 48 h. The assay was carried out in three replicates and the growth inhibition (%) was calculated compared with the control. The growth inhibition (%) was determined using the formula mentioned below:

$$\text{Growth inhibition (\%)} = \frac{(R - r)}{R} \times 100$$

Where: R is the diameter (mm) of growth in the control and r is the diameter of mycelial growth treated with AgNPs or Ag-CS-NCs.

Scanning electron microscopy imaging of *A. flavus*:

The scanning electron microscopy (SEM) imaging for the treated *A. flavus* isolates was performed using JEOL (JSM-7610F field emission SEM). The treated *A. flavus* isolates were prepared by the collected mycelium and fixed by solution containing formaldehyde (3%), in 0.05 M phosphate buffer solution (pH 6.8).

Samples were kept in this solution for two days, then washed three times for 20 min with distilled water and dehydrated with alcohol solution, then submitted to critical point drying according to Al-Othman *et al.* (2014).

Effect of AgNPs and Ag-CS-NCs on AFB1 production:

High performance liquid chromatography (HPLC) was used to quantify the determination of AFB1 (Gertz, 1990). 50 ml of SMKY liquid medium (20 g sucrose, 0.5 g magnesium sulphate, 3 g potassium nitrate, 7 g yeast extract in 1000 ml distilled water) were distributed into 100 ml Erlenmeyer flasks and autoclaved. A fungal disc of 5 mm diameter was transmitted in each 100 ml Erlenmeyer flask. Four different concentrations, 1 mL of AgNPs and Ag-CS-NCs (0.3, 0.5, 0.7 and 1 mM), each was added to SMKY liquid medium pre-inoculation with *A. flavus*, then incubated at ambient temperature (28°C) for 7 days with three replicates. To extract AFB1 in liquid cultures by methanol (80:20 methanol/liquid cultures) after separating mycelial mats. methanol was evaporated in a rotary evaporator under a vacuum at 35°C , dried residue containing AFB1 was dissolved in 1 ml of the solvent system. The solvent system was water: methanol: acetonitrile (60:20:20) and stored in dark vials. Before injection sample in HPLC, the sample was passed through a 0.45- μm micro-filter. Analysis of AFB1 was performed by HPLC (Perkin Elmer model series 200 UV/VIS) with a C18 column. 10 μl were used to inject (three replicates) and the quantification of AFB1 was calculated by the peak height. The HPLC system was equipped with a UV detector at 365 nm. The mobile phase (solvent system) was demonstrated in the previous paragraph. The total run time for the separation was approximately 25 min at a flow rate of 1 mL/min. The efficacy ratios (ER) for AFB1 inhibition were calculated using the equation below (Velluti *et al.*, 2003).

$$\text{Efficacy Ratios (ER)\%} = \frac{\text{AFB1 conc. in control} - \text{AFB1 conc. in treatment}}{\text{AFB1 conc. in control}} \times 100$$

RESULTS AND DISCUSSION

Biogenic synthesis of AgNPs and Ag-CS-NCs:

Figure 1A. shows pure aqueous solution AgNO_3 as control with yellow color, and the other screw bottle is colloid solutions of AgNPs (dark brown color). Figure 1B. reveals that the solution of reaction mixture included AgNO_3 and CS to production of Ag-CS-NCs (light brown color).

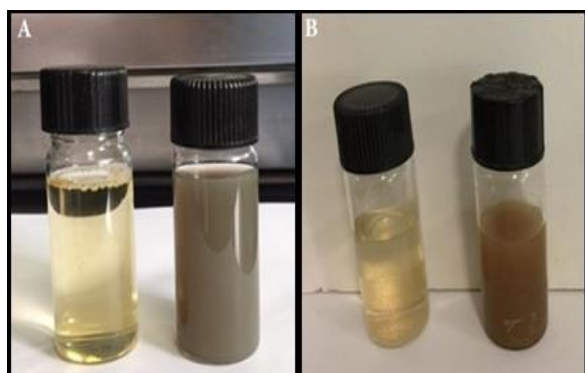


Figure (1): A) left screw bottle is aqueous solution AgNO_3 (control), right screw bottle is colloid solutions of AgNPs, B) left screw bottle is aqueous solution AgNO_3 (control), right screw bottle is colloid solutions of Ag-CS-NCs.

Previous literatures indicated a requirement for polymeric layers around AgNPs, in which AgNPs were finely distributed inside a polymeric matrix or coated with polymer to produce a core-shell structure (Choi and Luo, 2009; Levin *et al.*, 2009). In this work, chitosan was used as a polymer matrix for AgNPs to support Ag-CS-NCs production. In addition to promising features such as a formation smooth chain structure that allows for the integration of AgNPs, chitosan is renowned as a reducing and stabilizing agent for the green synthesis of Ag-CS-NCs (Thomas *et al.*, 2009). Silver ions are being regulated by amino groups of polymer

chains of chitosan supported by the acidic solution. Iron reduction to metallic AgNPs is coupled with oxidation of hydroxyl groups of chitosan. The reduction of silver ions to silver nanoparticles is related to the oxidation of chitosan's hydroxyl group (Regiel *et al.*, 2013). As a result, the polymeric nanocomposite system was established based on a chitosan network to produce Ag-CS-NCs. The stabilization of Ag-CS-NCs is attributed to the chemical bond between the electron-rich nitrogen found in the amino groups of chitosan and the silver orbitals through their ionic pairs (Kumar, 2000).

UV-Visible spectroscopy:

The formation of AgNPs in solution was monitored by using UV-vis spectral analysis. UV-vis spectral analysis depends on surface plasmon resonance (SPR), which is an optical phenomenon caused by light interacting with nanoparticles, in our case SPR showed an absorbance peak at 425 nm (Figure 2A) for AgNPs. Two significant peaks were observed at UV-Vis absorbance spectra of Ag-CS-NCs at various concentrations of NaOH (Figure 2B). The first peak at 275 nm was a characteristic peak of chitosan, whereas the second peak at 425 nm was a characteristic peak of nanosilver particles. Our results are confirmed by other researchers, the absorption peaks at 240 nm and 420 nm are unique surface plasmon resonance (SPR) for chitosan and AgNPs (Wang *et al.*, 2015; Ansari *et al.*, 2018).

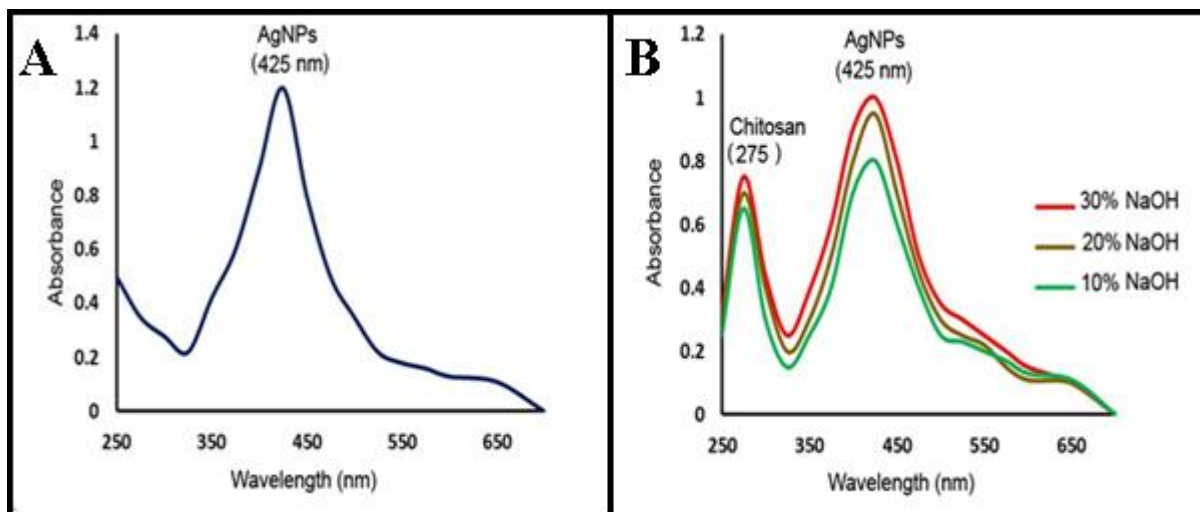


Figure (2): The UV-Vis absorbance spectra of the biogenic synthesized A) AgNPs, B) Ag-CS-NCs at various concentrations of NaOH solution.

Transmission electron microscopy (TEM):

Figure 3A illustrates the TEM micrograph with the frame of spherical or nearly spherical of AgNPs and without any significant agglomeration, also the particle size histogram

(Figure 3B) of AgNPs shows that the particle size ranges from 10 to 60 nm. 73% of all AgNPs size between 5 to 60 nm. Figure 4A shows the TEM image with the same features in the morphology and size of Ag-CS-NCs but differs in 75% of all

Ag-CS-NCs among 10 to 60 nm (Figure 4B). The particle size distribution of silver-incorporated chitosan nanocomposites (Ag@CS) was found to be 12-32 nm in diameter. Ag@CS particles were spherical in shape, well separated, and moderately dispersed (Le *et al.*, 2019). The particles of chitosan-mediated silver nanoparticles (Cs@Ag NPs) have been spherical form. Cs@Ag size distribution ranged from 10 to 60 nm. Most of the NPs showed the same size,

while only a few NPs larger than 60 nm (Kalaivani *et al.*, 2018). The presence of AgNPs on chitosan-based networks is clearly to production chitosan–silver nanocomposites (CS-HDA-AgNCs), and the average particle size of CS-HDA-AgNCs ranges between 2 and 50 nm (Palem *et al.*, 2018). In different results, Ag@CS was found to be 12-32 nm in diameter. Ag@CS were spherical in shape, well separated, and moderately dispersed (Le *et al.*, 2019).

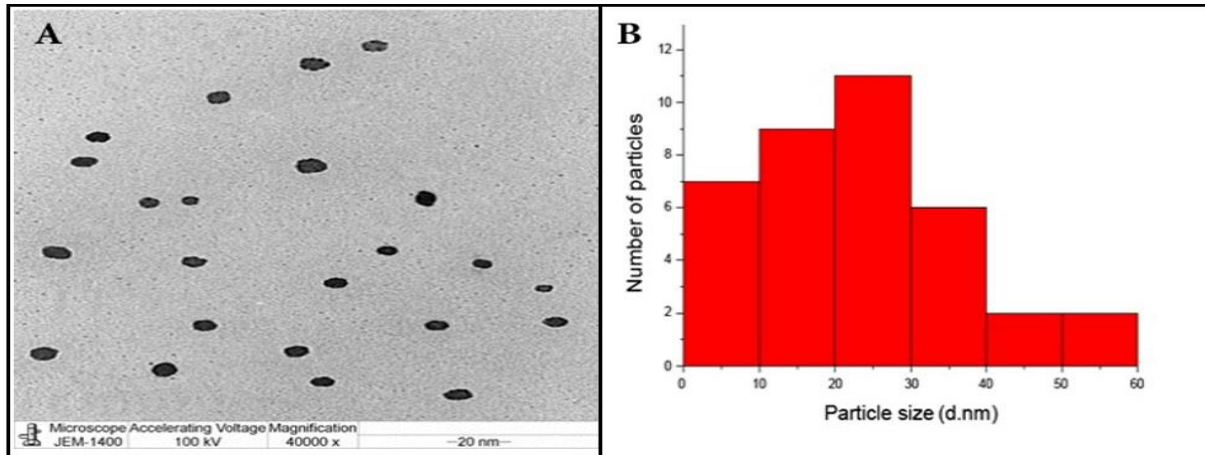


Figure (3): (A) TEM image of synthesized AgNPs by *Aspergillus terreus* (KC462061), (B) a particle size distribution histogram of synthesized AgNPs determined from TEM images

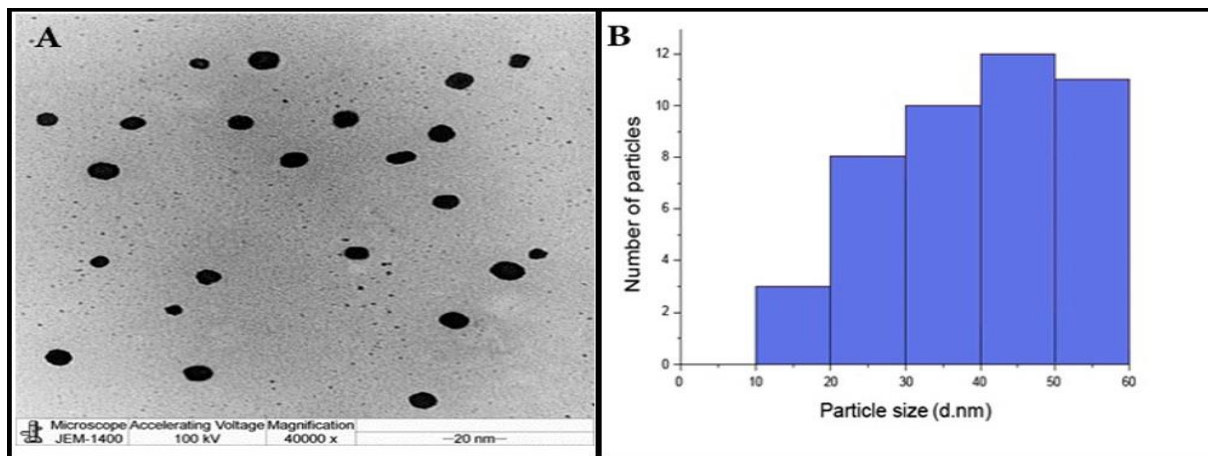


Figure (4): (A) TEM image of synthesized Ag-CS-NCs, (B) a particle size distribution histogram of synthesized Ag-CS-NCs determined from TEM images

The surface morphology, size, and elemental analysis:

The surface morphology, size, and elemental analysis of nanomaterials of pure AgNPs and Ag-CS-NCs were analyzed using HR-SEM and EDS and the images are described in Figure 5. The HR-SEM micrographs revealed a rough surface with uneven surface topology and heterogenous shape of the AgNPs (Figure 5A) also, the size less than 100 nm. For the knowledge of fundamental elements present in the synthesized AgNPs, EDS analysis was performed (Figure 5B). The results showed the presence of silver, potassium and

chloride in synthesized AgNPs. It was apparent from the EDS profile that the mass percent of elemental silver was very high in AgNPs (80%). EDS data also conferred many strong signals of silver, with weak signals for other elements. Figure 5C shows quantitative of elements formed AgNPs. As shown in Figure 6, the surface morphology of the Ag-CS-NCs is a thin, straight and smooth pipe with homogeneous structure with a several layers. EDS analysis (Figure 6B) shows the presence of silver, carbon, oxygen, potassium, and aluminum in synthesized Ag-CS-NCs. Figure 6C shows quantitative of elements

formed Ag-CS-NCs. The mass percent of elemental silver was about 80% based on EDS data, meaning elemental silver was very establish and powerful in both nanomaterials. SEM photographs of the biosynthesized silver nanoparticles–chitosan composite (Ag/CS/NCs) were homogeneous, smooth and relatively spherical in shape (Wang *et al.*, 2015; Palem *et al.*, 2018; Raza *et al.*, 2021). Interestingly, in

another study SEM images of chitosan-silver nanocomposites (CS/Ag/NCs) revealed a branching structure similar to the flower structure (Kumar-Krishnan *et al.*, 2015). EDS spectra proved the significant presence of pure metallic Ag with the presence of carbon and oxygen (with medium intensity). This confirms that chitosan undergoes crosslinking with metallic Ag nano (Palem *et al.*, 2018; Wang *et al.*, 2015).

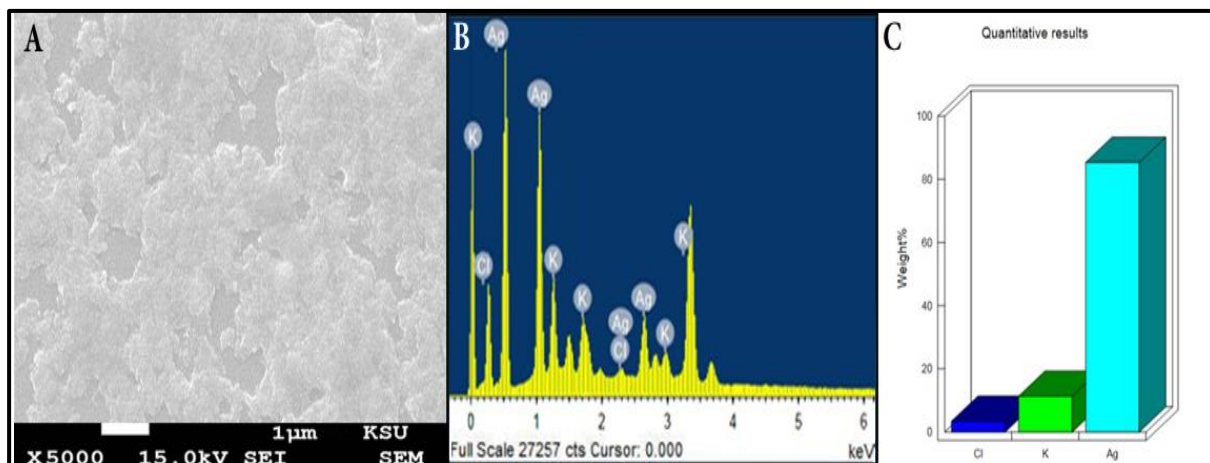


Figure (5): (A) SEM image of synthesized AgNPs, (B) EDS micrograph, (C) quantitative of elements formed AgNPs from TEM images

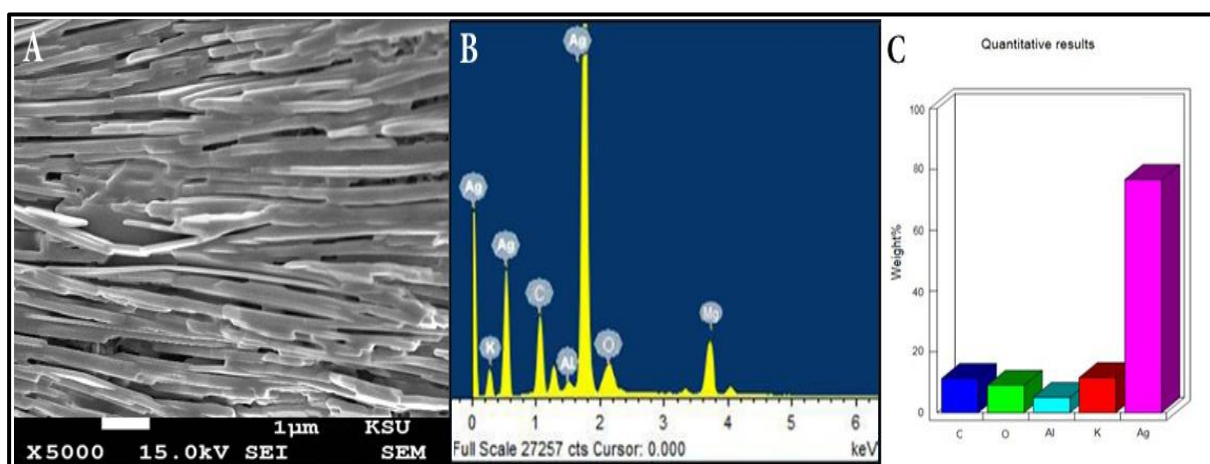


Figure (6): (A) SEM image of synthesized Ag-CS-NCs, (B) EDS micrograph, (C) quantitative of elements formed Ag-CS-NCs from TEM images

Spectroscopy of the fourier transform infrared (FTIR):

FT-IR spectra was used to identify the potential functional groups in the fungal extract that are responsible for the bioreduction of Ag ions and the production of AgNPs and Ag-CS-NCs. FTIR in Figure 7 shows spectra of AgNPs (7a) and Ag-CS-NCs (7b). There were no significant peaks in the regions $3500\text{--}4000\text{ cm}^{-1}$ and $2000\text{--}3000\text{ cm}^{-1}$ for biosynthesized nanoparticles spectra. In this analysis, the bands defined strenuous vibrations that were responsible for compounds such as flavonoids,

phenols, terpenoids and proteins, to be a valuable tool for the characterization and identification of compounds or functional groups, and the spectra of pure compounds are usually so unique that they are like a molecular fingerprint (Rauwel *et al.*, 2015) Which may suggest that the reduction, capping which stabilization of the AgNPs and Ag-CS-NCs were responsible for these biomolecules in the extracts (Mehmood *et al.*, 2016). AgNPs FTIR spectra included the broad and intense peak at 3440 cm^{-1} can be attributed to the stretching of -OH group (phenolic compounds) due to interaction between these

phenolic compounds and Ag^+ to form intermediate compounds which would undergo oxidation and thus reduction of Ag^+ to form AgNPs (Malik *et al.* 2014; Deenadayalan *et al.*, 2014). The band 1650 was revealed about C=C and was regularly related to amide I (C=O) and amide II (C-N-H), that corresponds to the band vibrations of proteins (Abd El-Aziz *et al.*, 2013). The band around 1445 cm and 1245 cm can be attributed to C-N stretching vibration of aliphatic and aromatic amines indicating the presence of amino acid (Abdel-Hafez *et al.*, 2016). Ag-CS-NCs FTIR spectra included the band at 2940 cm^{-1} corresponded to the alkane C-H-stretching lipids (Wang *et al.*, 2015). Shift of NH_2 of amide in Ag-CS-NCs spectra from 1650 cm^{-1} to 1627

cm^{-1} . This shift of 1627 cm^{-1} was observed and as result to Ag^+ loaded on Ag-CS-NCs spectra (Murugadoss and Chattopadhyay, 2008). The shift of $-\text{C}=\text{C}$ stretching vibration of aromatic amine in CS from 1581 cm^{-1} to 1499 cm^{-1} were detected in the spectrum of Ag-CS-NCs which assigned to primary and secondary amines bonds of proteins (Vidhu and Philip, 2014). The interactions of amine, hydroxyl as well as bending vibrations (1469 cm^{-1}) in Ag-CS-NCs seems slightly in intensity due to the crosslinker between AgNPs and N-H/O-H groups to obtain Ag-CS-NCs. Also, the formation of new peaks at 1231, 1162, 1155, 1010 cm, confirms chitosan crosslinked with AgNPs to appear Ag-CS-NCs (Palem *et al.*, 2018).

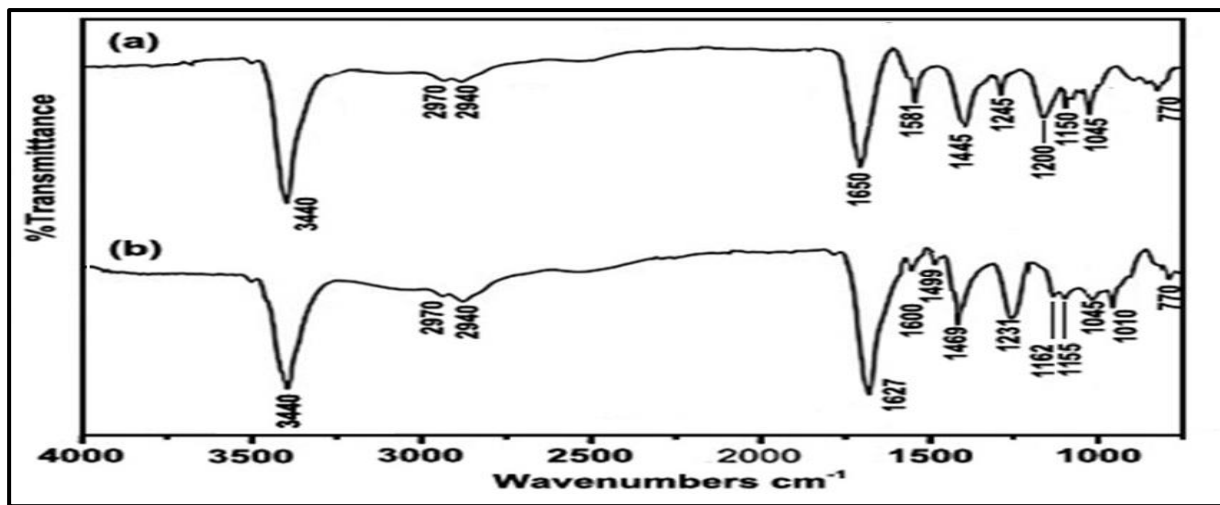


Figure (7): FTIR spectrum of synthesized a) AgNPs and b) Ag-CS-NCs

Antifungal Activity of Ag NPs and Ag-Chit-NCs Against *A. flavus*:

The colloidal solutions of AgNPs and Ag-Chit-NCs at various concentrations (0.3, 0.5, 0.7, 1 mM) were used to evaluate the inhibitory activity against *A. flavus*, high producer of B1 (C8), isolated from maize crop (Table 1). All tested concentrations of AgNPs and Ag-Chit-NCs were successful in growth inhibition of *A. flavus* through treatment duration. The inhibition growth (GI%) reached 71.87% and 75.0% in the case of treatment with a 1mM of AgNPs and Ag-Chit-NCs compared with the control. The small scale, larger surface area, and tunable surface chemistry of nanoparticles make them very ideal as a superior antifungal agent also could be used commercially level (Reidy *et al.*, 2013, Venkatesan *et al.*, 2016). The accurate mechanism of AgNPs by which the reaction occurs, however, is still largely unknown. Numerous researchers have investigated the electrostatic affinity between the cell membranes of negatively charged microorganisms and

positively charged AgNPs, resulting in disturbance of cell walls and, consequently, increase their permeability which is very important for the antimicrobial effect (Sánchez-López *et al.*, 2020). In biological molecules, nanoparticles bind to thiol ($-\text{SH}$) practical groups of proteins lead to denaturing proteins. Resulting in defects in the microbial cell membrane and intracellular material loss. The nanoparticles inhibit respiratory chain enzymes within the cells, contributing to the microbial cells' death (Prabhu and Poulse, 2012).

The antimicrobial activity of CS depends on the positively charged amino group and the interference with the negatively charged cell surface. Chitosan's structure contains active functional groups (amino and hydroxyl groups) that are known to have biocidal activities (Liu *et al.*, 2018). CS improved aggregate stability for AgNPs by its structure as polymers and surfactants against fungi with which presenting relatively high antifungal activity (Laudenslager *et al.*, 2008). However, some other factors could

have been effect on an antimicrobial activity such as 1) the molar mass 2) the size, density of the positive charge present, 3)

hydrophilicity/hydrophobicity and 4) the ionic strength of the chitosan used for the production of nanocomposite system (Kong *et al.*, 2010).

Table (1): Zone of inhibition (mm) of Ag NPs and Ag-Chit-NCs against *A. flavus* isolate isolated from corn grain

Conc. of nanoparticles	AgNPs		Ag-CS-NCs	
	Diameter of zone of inhibition (mm)	Growth inhibition %	Diameter of zone of inhibition (mm)	Growth inhibition %
0.3mM	17.0	46.87	13.0	59.37
0.5mM	16.0	50.00	9.5	70.31
0.7mM	13.5	57.81	11.0	65.62
1mM	9.0	71.87	8.0	75.00
Control	35.0	-	35.0	-
LSD at 0.05%	0.487	-	0.341	-

Fungal morphology via HR-SEM

The morphology structure of *A. flavus* was examined by HR-SEM after treatment with AgNPs and Ag-CS-NCs (Figure 8) with a focus on deformation and abnormal surface properties. Untreated mycelia (control) have normal shape of conidiophore and spores (Fig. 9A). Fungal treatment with AgNPs concentration at (0.3mM) showed a normal case of conidiophore and spores (Figure 8B). Treatment with Ag-CS-NCs (1mM) caused damage such as malformations of spores and unusual shape of conidiophore (Figure 8C), also reduce in spores' number (Figure 8D), SEM image of fungal spores showed disappearance, deformation and abnormal surface properties that lead to damage of spores (Figure 8E). Treatment of fungal hyphae with AgNPs (1mM) showed damages such as 1) deformations in the shape of conidiophores and the mature conidia and 2) unusual bulges and ruptures. Effects of AgNPs on the fungal spores were observed, damage such as reduce in spores' number, malformations and hypertrophy, these effects lead to the destruction of spores (Al-Othman *et al.*, 2014). SEM analysis of filamentous pathogenic fungi such as *Fusarium verticillioides*, *Penicillium citrinum* and *Aspergillus flavus* after treatment with gold nanoparticles (GNPs) 0.2 mg /L presented many damages as: deformations, broken and unusual bulges comparing with untreated (control) fungi (Savi *et al.*, 2012). AgNPs synthesized by *A. alternata* at the concentration 100 mg/L gave the highest inhibition zone against *Aspergillus flavus* and *Alternaria alternata*, where the percentages of reduction were 77.1 and 87.6%, respectively (Al-Zaban *et al.*, 2021). AgNPs, chitosan (CS), silver-chitosan nanocomposites Ag@CS and Ag@CS/An were used to growth inhibition of *Phytophthora capsici*. Ag@CS/An was observed to have significantly more powerful as an

antifungal capacity than each component alone. Ag@CS/An have many features like 1) cost saving, 2) safety and high antifungal effectiveness and 3) reducing the risk of environmental pollution also, it anticipated Ag@CS/An has a promising future as nano-antifungal materials for agricultural crops (Le *et al.*, 2019). Ag-CS-NCs were used as antifungal activity against *Antrodia cinnamomea* and *Cordyceps militaris*. This investigation shows a selective inhibition up to 85% or more by Ag-CS-NCs, suggesting that Ag-CS-NCs can be used for many applications such as fungicidal. Ag-CS-NCs were reported as a broad spectrum of antifungal activity (Wang *et al.*, 2015). Herein, SEM examination confirmed the harmful effect on fungal hyphae (*Colletotrichum gloeosporioides*) examined 72 hours after the treatment with 100 ppm AgNPs, showed malformations in mycelial growth and the form of hyphal walls. The layers of hyphal walls were also torn off on damaged hyphae (Lamsal *et al.*, 2011).

Effect of AgNPs and Ag-CS-NCs on AFB1 production:

Figure 9 shows HPLC chromatogram of AFB1 (control) and treated with AgNPs and Ag-CS-NCs at concentration of 1mM to study their effect on AFB1 production. The efficiency ratios of AFB1 inhibition (ER%) values, shown in Table 2, indicate promising results for tested nanoparticles at various concentrations that were highly effective against AFB1 production Tables 2 and 3. ER% values of Ag-CS-NCs (1mM) were the highest significantly against AFB1 production also, 0.3mM were the smallest (79.65 and 52.41, respectively). ER% values of AFB1 inhibition of Ag-CS-NCs ranged from 52.41 to 79.65 %, while, ER% values of Ag NPs were ranged between 51.37 to 70.68 %.

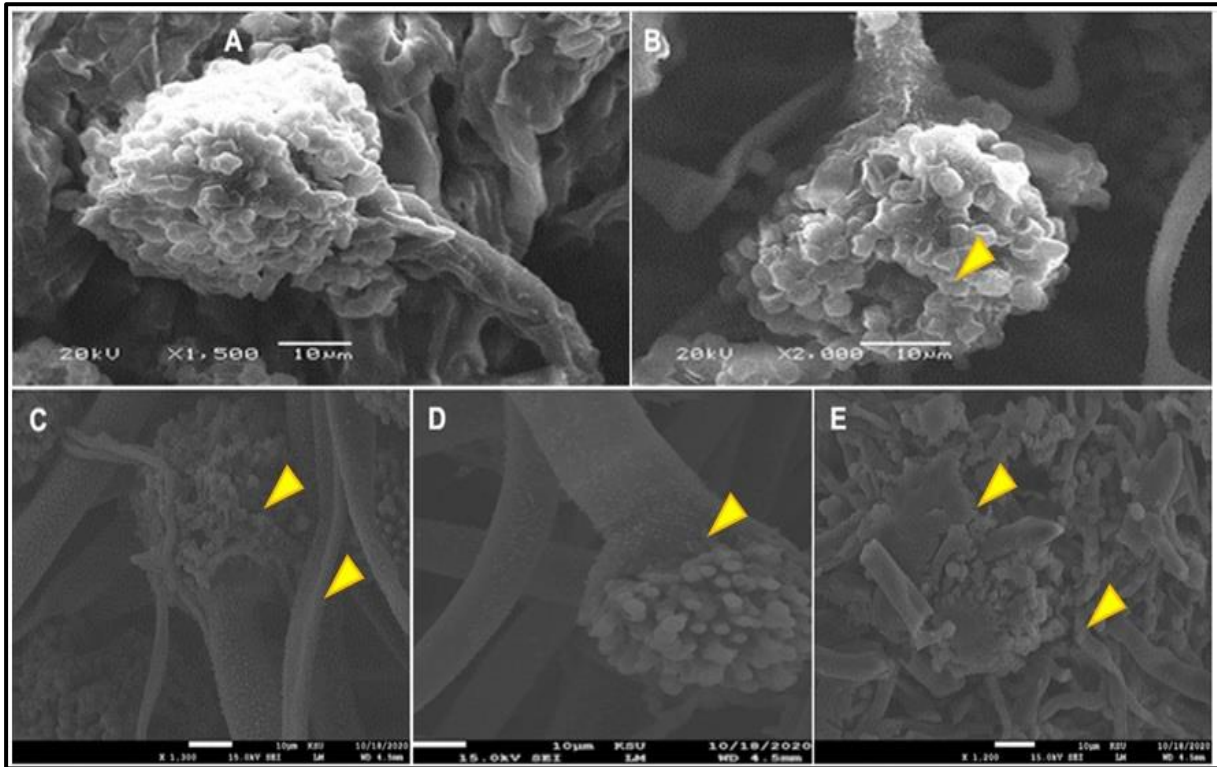


Figure (8): SEM images of *A. flavus*, control without treatment (A), AgNPs (0.3mM) (B) and treatment with Ag-CS-NCs (1mM) (C, D, E).

Table (2): Effect of the applied AgNPs on AFB1 concentration and the efficacy ratio of AFB1 production inhibition (ER%) for the three tested isolates C12, C6 and C8 of *A. flavus*.

Conc. of nanoparticles	C12		C6		C8	
	Conc.	Efficacy Ratios (ER)	Conc.	Efficacy Ratios (ER)	Conc.	Efficacy Ratios (ER)
0.3mM	0.51	63.57	1.25	45.65	1.41	51.37
0.5mM	0.39	72.14	1.12	51.30	1.26	56.55
0.7mM	0.27	80.71	0.89	61.69	0.93	67.93
1mM	0.19	86.42	0.61	73.47	0.85	70.68
Control	1.40	-	2.30	-	2.90	-
LSD at 0.05%	0.105	-	0.114	-	0.217	-

Table (3): Effect of the applied Ag-CS-NCs on AFB1 concentration and the efficacy ratio of AFB1 production inhibition (ER%) for the three tested isolates C12, C6 and C8 of *A. flavus*.

Conc. of nanoparticles	C12		C6		C8	
	Conc.	Efficacy Ratios (ER)	Conc.	Efficacy Ratios (ER)	Conc.	Efficacy Ratios (ER)
0.3mM	0.46	67.14	1.19	48.26	1.38	52.41
0.5mM	0.32	77.14	1.06	53.56	1.17	59.65
0.7mM	0.21	84.28	0.59	74.34	0.77	73.44
1mM	0.15	89.28	0.39	83.04	0.59	79.65
Control	1.40	-	2.30	-	2.90	-
LSD at 0.05%	0.125	-	0.196	-	0.171	-

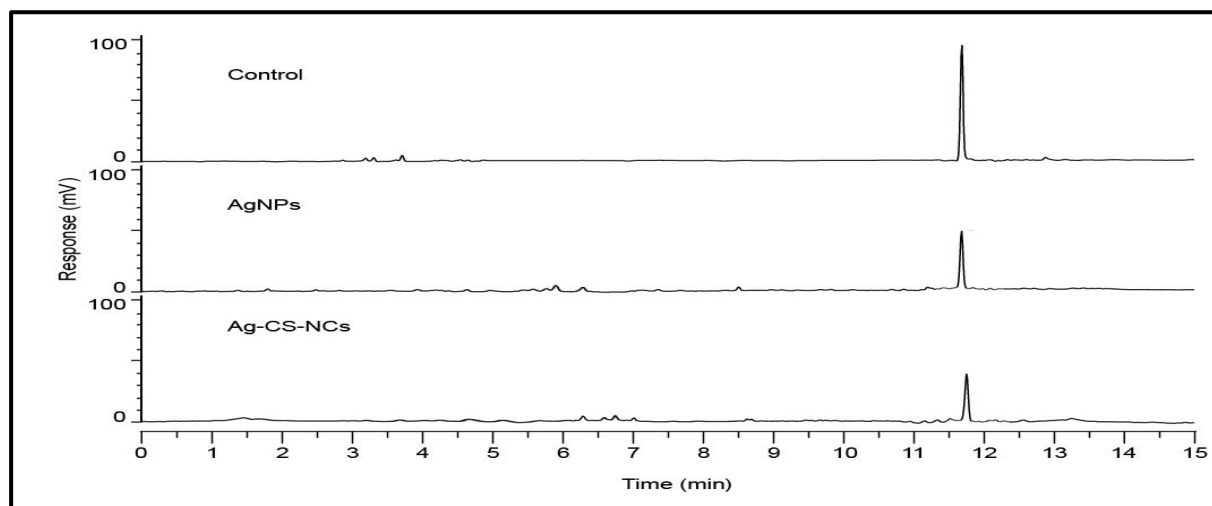


Figure (9): HPLC chromatogram of AB1 production and treatment with Ag NPs and Ag-CS-NCs 1mM.

REFERANCES

- Abdallah, M.F.; Ameye, M.; De Saeger, S.; Audenaert, K. and Haesaert, G. 2018. Biological control of mycotoxigenic fungi and their toxins: An update for the pre-harvest approach. In *Fungi and Mycotoxins-Their Occurrence, Impact on Health and the Economy as Well as Pre- and Postharvest Management Strategies*; Berka Njobeh, P., Ed.; Intech Open: London, UK.
- Abd El-Aziz, A.R.M.; Al-Othman, M.R.; Eifan, S.A.; Mahmoud, M.A. and Majrashi, M. 2013. Green synthesis of silver nanoparticles using *Aspergillus terreus* (KC462061). *Dig. J. Nanomater. Biostruct.* 8: 1215-1225.
- Abdel-Hafez, S.I.; Nafady, N.A.; Abdel-Rahim, I.R.; Shaltout, A.M.; Daros, J.A. and Mohamed, M.A. 2016. Assessment of protein silver nanoparticles toxicity against pathogenic *Alternaria solani*. *3 Biotech*, 6: 199.
- Al-Othman, M.R.; Abd El-Aziz, A.R.M.; Mahmoud, M.A.; Eifan, S.A.; El-Shikh, M.S. and Majrashi, M. 2014. Application of silver nanoparticles as antifungal and antiaflatoxin B1 produced by *Aspergillus flavus*. *Dig. J. Nanomater. Biostruct.* 9 (1): 151-157.
- Al-Zaban, M.I.; Mahmoud, M.A. and Alharbi, M.A. 2021. A polyphasic approach to the characterization of potential silver nanoparticles-producing and non-producing isolates of *Alternaria* species and antifungal activity against mycotoxigenic fungi. *Biotechnology & Biotechnological Equipment*, 35:(1): 341-353.
- Ansari, A.; Sidra P.; Javed U.; Abro M.I.; Nawaz M.A.; Qader S.A. and Aman, A. 2018. Characterization and interplay of bacteriocin and exopolysaccharide mediated silver nanoparticles as an antibacterial agent. *Int. J. Biol. Macromol.* 115: 643-650.
- Balaure, P.C.; Gudovan, D. and Gudovan, I. 2017. Nanopesticides: A new paradigm in crop protection. *new Pestic. Soil Sens*, 129-192.
- Choi, Y. J. and Luo, T.J.M. 2009. Self-Assembly of silver-amino silica nanocomposites through silver nanoparticle fusion on hydrophobic surfaces. *ACS Appl. Mater. Interfaces.* 1: 2778-2784.
- Deenadayalan, A.K.; Palanichamy, V. and Selvaraj, M.R. 2014. Green synthesis of silver nanoparticles using *Alternanthera dentata* leaf extract at room temperature and their antimicrobial activity. *Spectrochim. Acta Part A Mol. Biomol. Spectrosc.* 127: 168-171.
- Gertz, C. 1990. *HPLC Tips and Tricks*. Great Britain at the Iden Press, Oxford. 608 pp.
- Ghormade, V.; Deshpande, M.V. and Paknikar, K.M. 2011. Perspectives for nano biotechnology enabled protection and nutrition of plants. *Biotechnol. Adv.* 29: 792-803.
- Griffiths, P.R. and de Haseth, J.A. 2007. *Fourier Transform Infrared Spectrometry*. John Wiley & Sons, INC., Publication, 2007, 2nd Ed. 560 pp.
- Jung, J.; Kasi, G. and Seo, J. 2018. Development of functional antimicrobial papers using chitosan/starch-silver nanoparticles. *Int. J. Biol. Macromol.*, 112: 530-536.
- Kalaivani, R.; Maruthupandy, M.; Muneeswaran, T.; Beevi, A.H; Anand, M.; Ramakritinan, C.M. and Kumaraguru, A.K. 2018. Synthesis of chitosan mediated silver nanoparticles

- (AgNPs) for potential antimicrobial applications. *Frontiers in Laboratory Medicine*, 2: (1): 30-35.
- Kaur, P.; Thakur, R. and Choudhary, A. 2012. An in vitro study of the antifungal growth of silver/chitosan nanoformulations against important seed borne pathogens. *Int. J. Sci. Technol. Res.* 1: 83-86.
- Kim, D.Y.; Kadam, A.; Shinde, S.; Saratale, R.G.; Patra, J. and Ghodake, G. 2018. Recent developments in nanotechnology transforming the agricultural sector: A transition replete with opportunities. *J. Sci. Food Agric.* 98: 849-864.
- Kong, M.; Chen, X.; G.; Xing, K. and Park, H.J. 2010. Antimicrobial properties of chitosan and mode of action: a state-of-the-art review. *Int. J. Food Microbiol.* 144: 51-63.
- Kumar, M.N.R. 2000. A review of chitin and chitosan applications. *React. Funct. Polym.* 46: 1-27.
- Kumar-Krishnan, S.; Prokhorov, E.; Hernández-Iturriaga, M.; Mota-Morales, J.D., Vázquez-Lepe, M.; Yuri, K.; Isaac, C. and Sanchez, G.L. 2015. Chitosan/silver nanocomposites: Synergistic antibacterial action of silver nanoparticles and silver ions. *European Polymer Journal*, 67: 242-251.
- Lamsal, K.; Kim, S.W.; Jung, J.H.; Kim, Y.S.; Kim, K.S. and Lee, Y.S. 2011. Application of silver nanoparticles for the control of *Colletotrichum* species in vitro and pepper anthracnose disease in field. *Mycobiology*, 39(3): 194-199.
- Laudenslager, M.J.; Schiffman, J.D. and Schauer, C.L. 2008. Carboxymethyl chitosan as a matrix material for platinum, gold, and silver nanoparticles. *Biomacromolecules*, 9(10): 2682-2585.
- Le, V.T.; Bach, L.G.; Pham, T.T.; Le, N.T.T.; Ngoc, U.T.P.; Tran, D.N. and Nguyen, D.H. 2019. Synthesis and antifungal activity of chitosan-silver nanocomposite synergize fungicide against *Phytophthora capsica*. *Journal of Macromolecular Science, Part A*, 56: 1-8.
- Levin, C.S.; Hofmann, C.; Ali, T.A.; Kelly, A.T.; Morosan, E.; Nordlander, P.; Whitmire, K.H. and Halas, N.J. 2009. Magnetic-plasmonic core-shell nanoparticles. *ACS Nano*. 3: 1379-1388.
- Li, Z.; Lin, S.; An, S.; Liu, L.; Hu, Y. and Wan, L. 2019. Preparation, characterization and Anti-Aflatoxigenic activity of chitosan packaging films incorporated with turmeric essential oil. *Int. J. Biol. Macromol.* 131: 420-434.
- Liu, X.; Jiang, Q. and Xia, W. 2018. One-step procedure for enhancing the antibacterial and antioxidant properties of a polysaccharide polymer: Kojic acid grafted onto chitosan. *Int. J. Biol. Macromol.* 113: 1125-1133.
- Mahmoud, M.A.; Ali, H.M.; Abd El-Aziz, A.R.M.; Al-Othman, M.R. and Al-Wadai, A.S. 2014. Molecular characterization of aflatoxigenic and non-aflatoxigenic *Aspergillus flavus* isolates collected from corn grains. *Genet. Mol. Res.* 13 (4): 9352-9370.
- Malik, P.; Shankar, R.; Malik, V.; Sharma, N. and Mukherjee, T.K. 2014. Green chemistry based benign routes for nanoparticle synthesis. *J. Nanopart.* 24: 1-14.
- Mehmood, R.A.; Murtaza, G.; Bhatti, T.M.; Kausar, R. and Ahmed, M.J. 2016. Biosynthesis, characterization and antimicrobial action of silver nanoparticles from root bark extract of *Berberis lyceum*. *Pak. J. Pharm. Sci.* 29: 131-137.
- Murugadoss, A. and Chattopadhyay, A. 2008. A green chitosan silver nanoparticle composite as a heterogeneous as well as micro-heterogeneous catalyst. *Nanotechnology*, 19(1): 1-9, Article ID 015603.
- Musarrat, J.; Dwivedi, S., Singh, B.R.; Al-Khedhairi, A.A; Azam, A. and Naqvi, A. 2010. Production of antimicrobial silver nanoparticles in water extracts of the fungus *Amylomyces rouxii* strain KSU-09. *Bioresour Technol.* 101(22): 8772-8776.
- Omeiza, G.K.; Kabir, J.; Kwaga, J.K.P.; Kwanashie, C.N.; Mwanza, M. and Ngoma, L. 2018. A Risk assessment study of the occurrence and distribution of aflatoxigenic *Aspergillus flavus* and aflatoxin B1 in dairy cattle feeds in a central northern State, Nigeria. *Toxicol. Rep.* 5: 846-856.
- Palem, R.R.; Saha, N.; Shimoga, G.D.; Kronekova, Z.; Sláviková, M. and Saha, P. 2018. Chitosan-silver nanocomposites: New functional biomaterial for health-care applications. *Int. J. Polym. Mater.* 67(1): 1-10.
- Prabhu, S. and Poulouse E.K. 2012. Silver nanoparticles: mechanism of antimicrobial action, synthesis, medical applications, and toxicity effects. *Int. Nano. Lett.* 2(32): 1-10.
- Rauwel, P.; Küünaal S.; Ferdov, S. and Rauwel, E. 2015. A review on the green synthesis of silver nanoparticles and their morphologies studied via TEM. *Adv. Mater. Sci. Eng.* Article ID 682749.

- Raza, S.; Ansari, A.; Siddiqui, N.N.; Ibrahim, F.; Abro, M.I. and Aman, A. 2021. Biosynthesis of silver nanoparticles for the fabrication of non-cytotoxic and antibacterial metallic polymer-based nanocomposite system. *Sci. Rep.*,11, 10500.
- Regiel, A.; Kyzioł, A. and Arruebo, M. 2013. Chitosan-silver nanocomposites-modern antibacterial materials. *Chemik*, 67: 683-92.
- Reidy, B.; Haase, A.; Luch, A.; Dawson, K. A. and Lynch, I. 2013. Mechanisms of silver nanoparticle release, transformation and toxicity: a critical review of current knowledge and recommendations for future studies and applications. *Materials*, 6(6): 2295-2350.
- Sadowski, Z.; Maliszewska, H.I.; Grochowalska, B.; Polowczyk, I. and Kozlecki, T. 2008. Synthesis of silver nanoparticles using microorganisms, *Materials Science-Poland*, 26(2):419-424.
- Sánchez-López, E.; Gomes, D.; Esteruelas, G.; Bonilla, L.; Lopez-Machado, A. L.; Galindo, R.; Amanda, C.; Marta, E.; Miren, E.; Antoni, C.; Amélia, M.S.; Alessandra, D.; Antonello, S.; Maria, L.G. and Eliana, B.S. 2020. Metal-based nanoparticles as antimicrobial agents: An Overview. *Nanomaterials*, 10(2): 292-331.
- Savi, G.D.; Paula, M.M.S.J.; Possato, C.; Barichello, T.; Castagnaro, D. and Scussel, V.M. 2012. Biological activity of gold nanoparticles towards filamentous pathogenic fungi. *Journal of Nano Research*, 20: 11-20.
- Stephenson, G.R. 2003. Pesticide Use and World Food Production: Risks and Benefits; ACS Publications: Washington, DC, USA, Chapter 15, pp 261-270.
- Thomas, V.; Yallapu, M.M.; Sreedhar, B. and Bajpai, S.K. 2009. Fabrication, characterization of chitosan/nanosilver film and its potential antibacterial application. *J. Biomater. Sci. Polym. Ed.*, 20(14): 2129-2144.
- Velluti, A.; Sanchis, V.; Ramos, A.J.; Egidio, J. and Marin, S. 2003. Inhibitory effect of cinnamon, clove, lemongrass, oregano and palmarose essential oils on growth and fumonisin B1 production by *Fusarium proliferatum* in maize grain. *Int. J. Food Microbiol.* 89: 145-154.
- Venkatesan, J.; Kim, S. and Shim, M.S. 2016. Antimicrobial, antioxidant, and anticancer activities of biosynthesized silver nanoparticles using marine algae *Ecklonia cava*. *Nanomater.*, 6(12): 235-253.
- Vidhu, V.K. and Philip, D. 2014. Spectroscopic, microscopic and catalytic properties of silver nanoparticles synthesized using *Saraca indica* flower, *Spectrochimica Acta Part A: Molecular and Biomolecular Spectroscopy*, 117(3): 102-108.
- Wang, L.; Wang, C.; Yang.; C.; Hsieh, C.; Chen, S.; Shen, C.; Wang J. and Huang K. 2015. Synthesis and anti-fungal effect of silver nanoparticles-chitosan composite particles. *Int. J. Nanomedicine*, 10: 2685-2696.
- Worrall, E.A.; Hamid, A.; Mody, K.T.; Mitter, N. and Pappu H.R. 2018. Nanotechnology for plant disease management, *Agronomy*, 8: 285-309.